^{1}H-NMR Resonance Assignments, Secondary Structure, and Global Fold of the TR_1C Fragment of Turkey Skeletal Troponin C in the Calcium-Free State†

Wendy A. Findlay and Brian D. Sykes*

Department of Biochemistry and MRC Group in Protein Structure and Function, University of Alberta, Edmonton, Alberta, Canada T6G 2H7

Received December 1, 1992

ABSTRACT: The TR_1C fragment of turkey skeletal muscle TnC (residues 12–87) comprises the two regulatory calcium binding sites of the protein. Complete assignments of the ^{1}H-NMR resonances of the backbone and amino acid side chains of this domain in the absence of metal ions have been obtained using 2D ^{1}H-NMR techniques. Sequential (i,i+1) and short-range (i,i+3) NOE connectivities define two helix–loop–helix calcium binding motifs, and long-range NOE connectivities indicate a short two-stranded β-sheet formed between the two calcium binding loops. The two calcium binding sites are different in secondary structure. In terms of helix length, site II conforms to a standard "EF-hand" motif with the first helix ending one residue before the first calcium ligand and the second helix starting one residue after the β-sheet. In site I, the first helix ends three residues before the first calcium ligand, and the second helix starts three residues after the β-sheet. A number of long-range NOE connectivities between the helices define their relative orientation and indicate formation of a hydrophobic core between helices A, B, and D. The secondary structure and global fold of the TR_1C fragment in solution in the calcium-free state are therefore very similar to those of the corresponding region in the crystal structure of turkey skeletal TnC [Herzberg, O., & James, M. N. G. (1988) *J. Mol. Biol. 203*, 761–779].

The binding of calcium to the protein troponin C (TnC)[1] triggers muscle contraction in vertebrate striated (skeletal and cardiac) muscle. A conformational change in TnC induced by calcium binding is transmitted via the rest of the troponin complex (TnI and TnT) to other proteins of the thin filament of muscle [as reviewed in Zot and Potter (1987)]. This modifies the interaction between the thick and thin filaments and ultimately results in muscle contraction. The nature of the conformational change in TnC and the mode of its transmission are not known in detail, since no pair of structures for TnC in the calcium-free and the calcium-bound form have been obtained to date.

Skeletal TnC has four calcium binding sites— two higher affinity sites which also bind magnesium and two lower affinity calcium-specific sites (Potter & Gergely, 1975). The two higher affinity sites have been localized to the C-terminal region of TnC and the two lower affinity sites to the N-terminal region (Leavis et al., 1978). The higher affinity binding sites are thought to always be occupied by calcium or magnesium in vivo and probably play a structural role. Binding of calcium to the two lower affinity sites provides the regulatory role (Sheng et al., 1990).

The structure of avian TnC determined by X-ray crystallography (Herzberg & James, 1985; Sundaralingam et al., 1985) defined two domains each comprising two helix–loop–helix calcium binding motifs joined by a long central helix. Each pair of calcium binding sites has a short β-sheet formed between the two calcium binding loops (Herzberg & James, 1988; Satyshur et al., 1988), and this has also been found for other helix–loop–helix-type calcium binding proteins [reviewed by Strynadka and James (1989)]. In both reported crystal structures of TnC, the two C-terminal binding sites are occupied by calcium, but the two N-terminal sites are unoccupied, probably due to the conditions required for crystallization. X-ray scattering experiments (Heidorn & Trewhella, 1988) indicate that in solution the protein is more compact, with the two domains closer to each other. This suggests that the long central helix may be flexible as has been found for calmodulin (Ikura et al., 1991a; Barbato et al., 1992), a calcium binding protein with a very similar structure to TnC (Babu et al., 1985; Ikura et al., 1992).

Chazin and co-workers (Akke et al., 1992; Skelton et al., 1990) have used NMR to obtain high-resolution solution structures of calbindin D_{9k}, a small calcium binding protein comprising two helix–loop–helix motifs, in the presence and in the absence of calcium. They observed only small structural changes upon calcium binding. Calcium binding to calbindin D_{9k} appears to have a much larger effect on the backbone dynamics since amide exchange and ^{15}N relaxation measurements indicate that the protein is much less flexible in the calcium-loaded form (Linse et al., 1990; Kördel et al., 1992). A larger structural change might be expected to accompany calcium binding to TnC since it is a regulatory protein.

On the basis of the crystal structure, Herzberg et al. (1986) have proposed that the conformational change in the N-terminal domain of TnC when calcium binds involves reorientation of the helices so that their relative positions would be more similar to those of the corresponding helices in the calcium-saturated C-terminal domain. Several previous studies using site-specific mutagenesis of residues in the N-domain of TnC are consistent with this proposal (Fujimori et al., 1990; Grabarek et al., 1990; Pearlstone et al., 1992). To fully test the model, it will be necessary to obtain the solution structure of the N-domain both in the calcium-free state, to verify that the observed structure was not influenced by the low pH required for crystallization or by crystal packing,

† This work was supported by the Medical Research Council of Canada and the Alberta Heritage Foundation for Medical Research (fellowship to W.A.F.).

[1] Abbreviations: TnC, troponin C; TR_1C fragment, residues 12–87 of turkey skeletal TnC; TR_2C fragment, residues 92–162 of turkey skeletal TnC; NMR, nuclear magnetic resonance; NOE, nuclear Overhauser enhancement; 1D, one dimensional; 2D, two dimensonal; NOESY, 2D NOE spectroscopy; COSY, correlated spectroscopy; DQF-COSY, double quantum filtered COSY; TOCSY, total correlation spectroscopy; SBTI, soybean trypsin inhibitor; EDTA, ethylenediaminetetraacetic acid; DSS, disodium 2,2-dimethyl-2-silapentane-5-sulfonate.

0006-2960/93/0432-3461$04.00/0

and in the calcium-saturated state, to verify the nature of the primary structural change. Ultimately the structure of intact TnC in solution and in the troponin complex will be required to determine the mode of transmission of this calcium-induced conformational change.

Several groups (Drabikowski et al., 1985; Drakenberg et al., 1987; Tsuda et al., 1988, 1990) have examined changes accompanying calcium and magnesium binding to TnC or its isolated domains using ^{1}H-NMR, but this work has been hampered since they could only assign a few resonances in this protein. Rosevear and co-workers (Brito et al., 1991; Krudy et al., 1992) have recently published some assignments for cardiac TnC, which differs from skeletal TnC in having one nonfunctional calcium binding site in the N-domain. In all these studies, the fairly large size of TnC (~162 residues) in conjunction with its highly helical nature makes it difficult to completely assign the ^{1}H-NMR resonances from 2D ^{1}H-NMR spectra. The homologous protein calmodulin has recently been fully assigned in the calcium-bound state by Ikura and co-workers but required the development and use of new three- and four-dimensional triple-resonance techniques with fully ^{15}N- and ^{13}C-labeled protein (Ikura et al., 1990, 1991a,b).

Troponin C can be cleaved by trypsin to yield two large fragments (Grabarek et al., 1981). The TR_1C fragment corresponds to residues 12–87 of the N-terminal domain of TnC and contains the two regulatory calcium binding sites, and the TR_2C fragment corresponds to the C-terminal domain of TnC. We have isolated and purified the TR_1C fragment of turkey skeletal muscle TnC and completed the sequential assignment of the backbone and almost all of the side chain ^{1}H-NMR resonances using 2D ^{1}H-NMR techniques. Using NOE data, we have determined the secondary structure and global fold of this domain in solution in the metal-free state, which is a first step in determining the conformational change which accompanies binding of calcium to TnC and in elucidating the sequence of events involved in muscle contraction.

MATERIALS AND METHODS

Sample Preparation. The TR_1C fragment of turkey skeletal TnC was prepared by dissolving 50 mg of TnC [purified as described in McCubbin et al. (1982)] in 5 mL of 50 mM NH_4HCO_3, 50 mM NaCl, and 5 mM $CaCl_2$. A 1:100 (w/w) ratio of TPCK-treated trypsin (Worthington Biochemical Corp.) to TnC was added. After incubation for 2 h at room temperature, a 10-fold excess of soybean trypsin inhibitor (Boehringer Mannheim) was added to stop the proteolysis. The sample was applied to a 350-mL (1.5 × 90 cm) G-50 gel filtration column equilibrated and eluted with 50 mM NH_4HCO_3. The first peak contains trypsin–SBTI complex, free SBTI, and uncleaved TnC. The second peak contains the TR_1C and TR_2C fragments. After the addition of 2 mM $CaCl_2$, the mixture of fragments was loaded onto a 50-mL (1.5 × 30 cm) phenyl-Sepharose column (Pharmacia, Uppsala, Sweden) which was washed with 400 mL of 50 mM NH_4HCO_3 and 2 mM $CaCl_2$ to elute the TR_2C fragment. The TR_1C fragment was eluted with 50 mM NH_4HCO_3 and 2 mM EDTA and then lyophilized. To obtain metal-free TR_1C, 5–10 mg of fragment was dissolved in 0.5 mL of 50 mM NH_4HCO_3 and 100 mM EDTA. This sample was applied to a 50-mL (1.5 × 30 cm) G-25 gel filtration column equilibrated and eluted with 50 mM NH_4HCO_3 and monitored at λ = 254 nm. The first peak contains metal-free TR_1C fragment and the second EDTA and residual metal ions. The TR_1C fragment was lyophilized and redissolved several times in distilled and deionized water to remove residual NH_4HCO_3. For NMR experiments, 5–10 mg of TR_1C fragment was dissolved in 0.5 mL of 10 mM KH_2PO_4/50 mM KCl at pH 6.4 in either 90% ^1H_2O/10% ^2H_2O or 100% ^2H_2O.

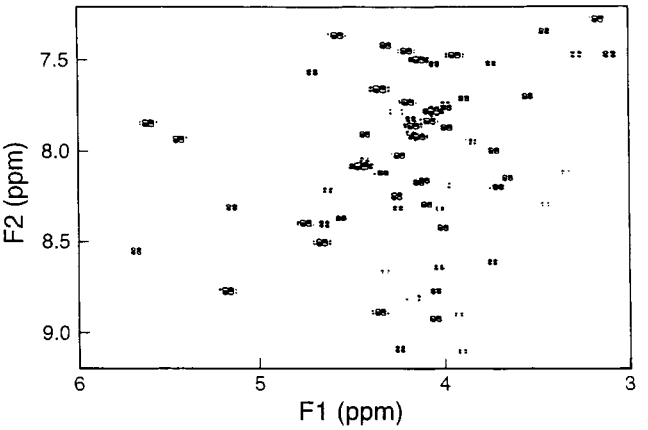

FIGURE 1: Fingerprint region (amide to α-hydrogens) of the 600-MHz DQF-COSY ^{1}H-NMR spectrum of 1.5 mM TR_1C fragment of turkey skeletal TnC in 10 mM KH_2PO_4, 50 mM KCl, and 10% ^2H_2O at pH 6.4 and 15 °C.

^{1}H-NMR Spectroscopy. All 1D spectra were acquired on a Varian Unity-500 spectrometer using a spectral width of 7000 Hz, a pulse width of 14.5 μs (90°), and an acquisition time of 2 s. The 2D spectra were acquired on a Varian Unity-600 spectrometer using a spectral width of 8000 Hz, a pulse width of 10.5 μs (90°), and an acquisition time of 0.128 s, collecting 2048 data points and 512 increments of 32 transients. Suppression of the ^1H_2O resonance was achieved using a 2.0–2.5-s presaturation pulse, and all spectra were referenced to the methyl resonance of DSS (internal standard) at 0 ppm. Scuba-NOESY (Brown et al., 1988) spectra with a mixing time of 150 ms, TOCSY spectra with a mixing time of 60 ms, and DQF-COSY spectra were acquired at 15 °C in both ^1H_2O and ^2H_2O buffers and used for the assignment of the ^{1}H-NMR resonances. The scuba-NOESY spectra were also used to determine the through-space connectivities used to define the secondary structure and the global fold. The slowly exchanging amide hydrogens were observed by acquiring a NOESY spectrum 1 h after redissolving the lyophilized sample in ^2H_2O.

The 2D data were processed on a SUN IPC workstation using the VNMR software package supplied by Varian. The data were zero-filled to 4K by 4K points for DQF-COSY spectra and to 4K by 2K points for TOCSY and NOESY spectra. Fairly high-resolution enhancement was applied, a line broadening of –10 Hz and a Gaussian function of 0.040 s in f_2 (the acquisition dimension), and a line broadening of –20 Hz and a Gaussian function of 0.015 s in the f_1 dimension.

RESULTS

The TR_1C fragment of turkey skeletal TnC (residues 12–87) has 76 residues of which 7 are glycines with 2 α-hydrogens and 1 is a proline with no amide hydrogen. The N-terminal amide hydrogens are expected to be in fast exchange with the solvent, so a maximum of 81 amide to α-hydrogen cross-peaks would be expected. In DQF-COSY spectra obtained at 15 °C and pH 6.4, we observed amide to α cross-peaks with varying intensity (see Figure 1) for 62 of the 76 residues, some of which could only be observed at very high vertical scale. The low intensity or absence of some COSY cross-peaks is a consequence of the small amide to α-hydrogen coupling constant for residues in an α-helical conformation. In NOESY spectra, we observed amide to α-hydrogen cross-

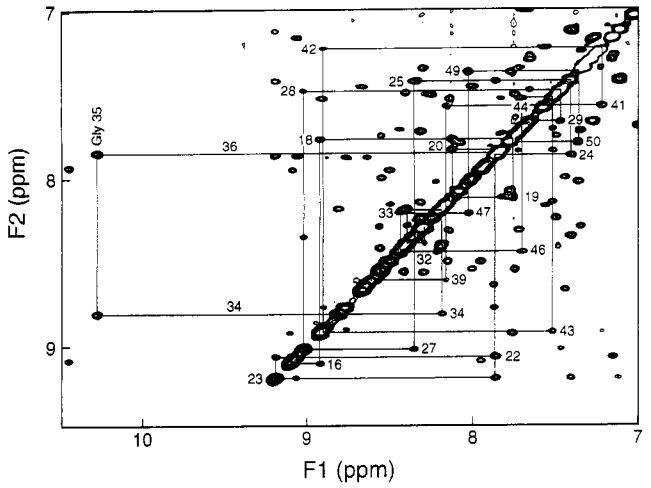

FIGURE 2: Amide region of the 600-MHz 2D ^{1}H-NMR NOESY spectrum of 1.5 mM TR_1C fragment in 10 mM KH_2PO_4, 50 mM KCl, and 10% ^2H_2O at pH 6.4 and 15 °C showing NH–NH(i,i+1) connectivities for calcium binding site I (residues 16–50).

peaks for all of the residues except the first two at the N-terminus. However, two pairs of CαH–NH cross-peaks (those of Glu21 and Ala24, and of Gln51 and Leu14) were found to be overlapping, and the CαH resonances of four residues (Asp30, Phe22, Ser38, and Ile73) are very close to the H_2O resonance, so become partially saturated during preirradiation of the solvent.

Sequence-Specific Assignments. The ^{1}H-NMR assignments were obtained using the strategies developed by Wüthrich and co-workers (Wagner & Wüthrich, 1982; Wüthrich, 1986). More than one-third of the residues could be easily classified by spin type. From DQF-COSY and TOCSY spectra in ^1H_2O and ^2H_2O, the six alanines, four threonines, seven glycines, and three of the four valines were identified as well as four AMX systems with CαH resonances downfield of the water peak. The CαH and CβH resonances of five of the six phenylalanines could be obtained from NOE cross-peaks from the aromatic region to the aliphatic hydrogen region since avian skeletal TR_1C has no tyrosines, tryptophans, or histidines.

The sequential assignment relied strongly on the large number of sequential NH–NH(i,i+1) cross-peaks observed in NOESY spectra of the TR_1C fragment in H_2O buffer. Because this polypeptide is largely helical, the sequence can be traced directly through these NH to NH cross-peaks, apart from the first two residues, the three residues involved in each strand of the short β-sheet between the calcium binding loops, and a break at Pro53. The tracing of the first calcium binding site (residues 16–50) is shown in Figure 2, and is complete apart from a break at Asp30 to Ala31, and from Asp36 to Ser38, where the residues are expected to be involved in the β-sheet. The CαH–NH(i,i+1) NOESY cross-peaks corresponding to the NH–NH(i,i+1) cross-peaks helped to confirm the sequential assignment, and these were supplemented by many CβH–NH(i,i+1) cross-peaks. A number of CαH–NH(i,i+3) cross-peaks characteristic of helical structure were also observed. The short- and medium-range NOE connectivities are summarized in Figure 3. The sequential assignment of the NH and CαH resonances of each residue was used to locate side chain resonances of many of the missing residues from TOCSY and/or COSY connectivities to the CαH resonance. We then checked that observed side chain resonances fit the expected spin system of each sequentially assigned residue to look for errors in the sequential assignment. The side chain assignments were obtained for the remaining residues apart from Lys23, as well as 3 of the 11 glutamic acids and 2 of the 7 methionines for which there is too much overlap in the 2D spectra (6 of the Glu's and 4 of the Met's have the CαH resonance in the range 4.0 ± 0.1 ppm, along with 8 other residues). We were able to completely assign three of the six Phe rings, but the other three did not exhibit enough chemical shift dispersion to allow them to be resolved.

The ^{1}H-NMR assignments for the TR_1C fragment in the absence of calcium are summarized in Table I. Previous assignments of 13 residues in the N-terminal domain of magnesium-saturated rabbit skeletal TnC by Tsuda et al. (1990) agree within 0.2 ppm for all resonances apart from those of Val62, which was not sequentially assigned in the previous work but which agrees almost perfectly with our assignment for Val45 (42 in the rabbit sequence). The peptide bond between Asn52 and Pro53 appears to be in the trans

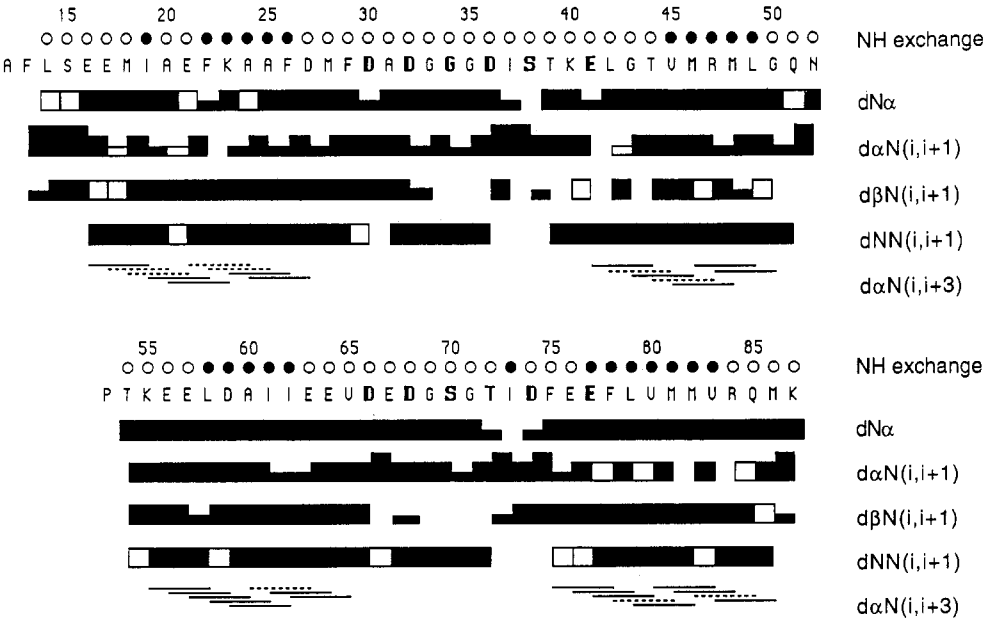

FIGURE 3: Sequential and short-range NOE connectivities observed for the TR_1C fragment. The height of the bar represents the relative strength of the NOESY cross-peak at a mixing time of 150 ms. Open bars and dashed lines indicate connectivities that were ambiguous because of overlap between resonances. Open circles above residues indicate amide hydrogens which exchange within 1 h of transfer of the polypeptide to ^2H_2O buffer, closed circles those which remain after 1 h. The calcium-liganding residues are shown in boldface type.

Table I: ^{1}H-NMR Chemical Shifts of the TR_1C Fragment of Turkey Skeletal TnC in the Absence of Calcium (pH 6.5, 15 °C)[a]

residue	no.	chemical shifts				
		NH	CαH	CβH/Cβ′H	CγH/Cγ′H	others
Ala	12		4.05	1.50		
Phe	13		4.60	3.07/3.01		7.23(δ)
Leu	14	8.08	4.46	1.50/1.28	1.49	0.77(δ&δ′)
Ser	15	7.91	4.44	4.0/4.0		
Glu	16	9.11	3.92	2.04	2.42/2.34	
Glu	17	8.93	4.06	2.04/1.94	2.41/2.29	
Met	18	7.76	3.99	1.96/1.63	2.30/2.08	
Ile	19	8.12	3.35	1.82	1.66	1.12(γCH$_3$), 0.79(δCH$_3$)
Ala	20	7.83	4.19	1.49		
Glu	21	7.86	4.18	2.28	2.53/2.43	
Phe	22	9.07	4.89	3.96/3.40		7.15(δ), 7.25(ε)
Lys	23	9.19	3.74	1.86		
Ala	24	7.86	4.18	1.52		
Ala	25	7.42	4.32	1.71		
Phe	26	8.36	3.66	3.25/2.74		6.62(δ), 6.94(ε), 7.49(ζ)
Asp	27	9.02	4.33	(2.73/2.63)		
Met	28	7.47	3.95	2.12	2.68/2.32	
Phe	29	7.66	4.35	3.22/2.45		7.29(δ)
Asp	30	7.26	4.89	2.85/2.24		
Ala	31	8.29	4.10	1.43		
Asp	32	8.40	4.75	2.83/2.70		
Gly	33	8.19	4.01/3.79			
Gly	34	8.81	4.18/3.91			
Gly	35	10.28	4.35/3.80			
Asp	36	7.85	5.62	2.55/2.49		
Ile	37	8.39	4.66	1.48	1.0/0.67	–0.16(γCH$_3$), 0.22(δCH$_3$)
Ser	38	8.68	4.91	4.14/3.75		
Thr	39	8.61	3.75	4.28	1.08	
Lys	40	8.17	4.15	1.84	1.48	1.70(δ,δ′), 3.0(ε,ε′)
Glu	41	7.56	4.72	1.89/1.58	2.35/2.14	
Leu	42	7.22	3.79	1.76/1.49	1.65	1.06&0.92(δ&δ′-CH$_3$)
Gly	43	8.92	3.77/3.50			
Thr	44	7.52	3.76	4.01	1.22	
Val	45	7.70	3.55	1.76	0.78&0.58	
Met	46	8.45	3.77	2.03		
Arg	47	8.22	4.62	1.95/1.92	1.90/1.82	3.29/3.19(δ/δ′)
Met	48	8.02	4.25	2.47/2.40	2.86/2.72	
Leu	49	7.36	4.58	1.73	1.87	1.09&0.88(δ&δ′-CH$_3$)
Gly	50	7.78	4.26/3.82			
Gln	51	8.08	4.45	1.58/1.52	2.16/1.99	6.99/7.68(NH$_2$)
Asn	52	8.77	5.18	2.74/2.52		6.78/7.58(NH$_2$)
Pro	53		4.75	2.15/2.00	1.94/2.01	3.26/3.65(δ,δ′)
Thr	54	8.89	4.36	4.75	1.36	
Lys	55	8.90	3.94	1.75	1.48/1.42	1.71(δ,δ′), 3.02(ε,ε′)
Glu	56	8.77	4.06	2.06		
Glu	57	7.87	4.00	2.35		
Leu	58	8.64	4.04	1.53	1.82	0.83&0.74(δ&δ′-CH$_3$)
Asp	59	8.67	4.33	2.74/2.63		
Ala	60	7.45	4.21	1.49		
Ile	61	8.00	3.74	2.02	0.99	0.89(γCH$_3$), 0.74(δCH$_3$)
Ile	62	8.55	3.45	1.91	1.84	0.94(γCH$_3$), 0.89(δCH$_3$)
Glu	63	7.74	4.00	2.08	2.41/2.30	
Glu	64	7.50	4.14	2.16/2.12	2.40	
Val	65	8.25	4.26	2.21	1.00&1.00	
Asp	66	8.32	5.15	2.92/2.26		
Glu	67	8.16	4.12	2.08/2.12	2.37/2.31	
Asp	68	8.50	4.67	2.88/2.73		
Gly	69	7.95	3.91/3.82			
Ser	70	9.09	4.25	4.05/3.97		
Gly	71	10.44	4.19/3.84			
Thr	72	7.94	5.45	4.00	1.02	
Ile	73	8.92	4.82	1.86	1.68/1.31	0.97(γCH$_3$), 0.91(δCH$_3$)
Asp	74	8.55	5.69	3.31/2.86		
Phe	75	8.42	3.53	2.66/2.46		6.43(δ), 7.22(ε), 7.41(ζ)
Glu	76	8.20	3.72	2.12	2.37/2.35	
Glu	77	8.42	4.02	2.45	2.70	
Phe	78	8.57	4.00	3.25/3.12		6.94(δ), 7.03(ε), 6.97(ζ)
Leu	79	8.30	3.46	1.55/1.26	1.14	0.77&0.72(δ&δ′-CH$_3$)
Val	80	7.35	3.45	2.17	1.05&0.90	
Met	81	7.71	3.90	2.00	2.45	
Met	82	8.32	4.04	1.75/1.95		
Val	83	8.15	3.67	2.09	1.05&0.89	
Arg	84	7.52	4.06	1.95	1.78/1.62	3.16(δ,δ′)
Gln	85	7.83	4.09	2.12/2.05	2.41/2.23	6.89/7.47(NH$_2$)
Met	86	7.73	4.21	2.21/2.07	(2.80/2.55)	
Lys	87	7.79	4.06	1.84/1.78	1.42	1.66(δ,δ′), 2.99(ε,ε′)

[a] Assignments are reported in ppm with respect to the methyl resonance of DSS; those listed in parentheses are tentative because of spectral overlap.

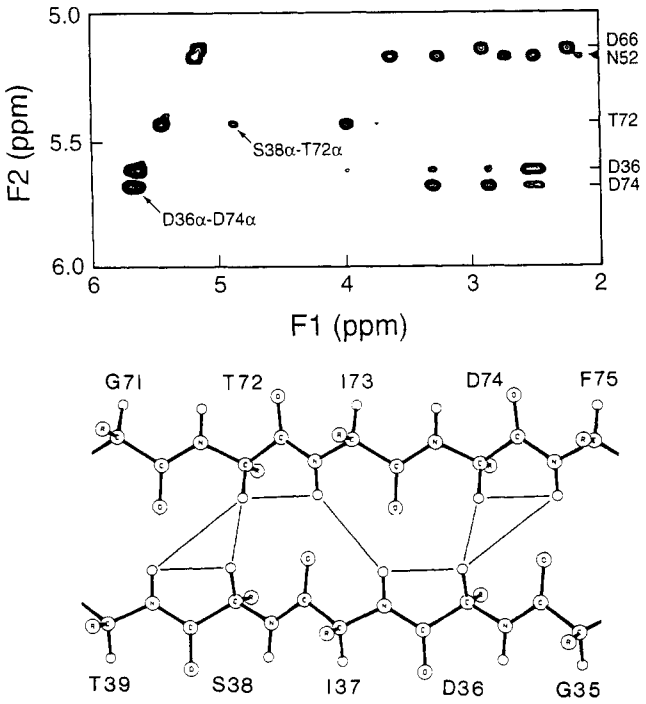

FIGURE 4: 600-MHz ^{1}H-NMR NOESY spectrum (top) of the TR_1C fragment showing residues with CαH resonances downfield of the H_2O signal. Cross-peaks between CαH resonances across the β-sheet are indicated. Schematic representation (bottom) shows all NOE connectivities observed between residues involved in the β-sheet between the two calcium binding loops.

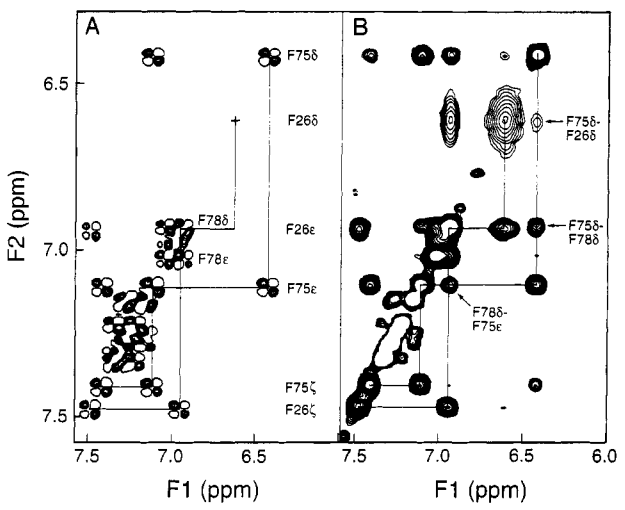

FIGURE 5: Aromatic region of 600-MHz 2D ^{1}H-NMR (A) DQF-COSY and (B) NOESY spectra of 1.5 mM TR_1C fragment in 10 mM KH_2PO_4, 50 mM KCl, and 100% ^2H_2O at pH 6.4 and 15 °C. The connections within the rings of Phe75, Phe78, and Phe26 are traced out, and NOESY cross-peaks between rings are indicated.

configuration since we observe strong NOE cross-peaks between the proline δ- and δ'-hydrogens and the CαH of the preceding asparagine. This is in contrast to calbindin D_{9k} which has a proline in the homologous position and exhibits cis–trans isomerization of the Gly–Pro peptide bond (Chazin et al., 1989).

Secondary Structure. The observed CαH–NH(i,i+3) NOE cross-peaks (Figure 3) indicate four helical regions for the TR_1C fragment—from Glu16 to Asp27, from Glu41 to Gly50, from Lys55 to Val65, and from Phe75 to Met86. This secondary structure is supported by the presence of slowly exchanging amide hydrogens for residues Phe22–Phe26, Val45–Leu49, Leu58–Ile62, and Glu77–Val83 (as shown in Figure 3), within each of the proposed helices. The NOESY spectrum of the region downfield of the H_2O peak is shown in Figure 4 (top). Resonances in this region corresponding to CαH hydrogens are characteristic of residues in the β-sheet (Wishart et al., 1991). We have identified Thr72, Asp36, and Asp74 with CαH resonances at 5.45, 5.62, and 5.69 ppm, respectively. Interstrand NOESY cross-peaks are observed between the CαH resonances of Asp36 and Asp74, and Ser38 and Thr72 as indicated in Figure 4. This figure also indicates the complete network of connectivities observed among these residues, which is consistent with formation of a short antiparallel β-sheet between residues Asp36 and Ser38 in site I and between Thr72 and Asp74 in site II.

The secondary structure is therefore the predicted pair of helix–loop–helix motifs joined by a short β-sheet expected for this class of calcium binding proteins, and in analogy with the crystal structure, we label the helices A, B, C, and D starting from the N-terminus of the fragment. However, the results summarized in Figure 3 suggest that the two calcium binding sites are significantly different. In calcium binding site I, helix A ends three residues before the first calcium ligand (Asp30), and helix B starts three residues after the β-sheet (Ser38), whereas in calcium binding site II, helix C ends one residue before the first calcium ligand (Asp66) and helix D starts right after the short β-sheet (Asp74). This difference in secondary structure may reflect further structural and/or functional differences between the two calcium binding sites.

Global Fold. The global fold adopted by the TR_1C fragment in solution is characterized by interactions between the helices which determine their relative orientation. Because of the helical nature of this polypeptide, there is a large degree of overlap of resonances, even in two-dimensional ^{1}H-NMR spectra. We were therefore able to assign long-range NOE connectivities unambiguously for only a few residues, mainly from side chain methyl and phenylalanine ring hydrogens, and could use these connectivities to obtain the global fold since the helices are fairly well defined.

The aromatic regions of COSY and NOESY spectra of the TR_1C fragment are shown in Figure 5. Resonances corresponding to the δ-hydrogens of Phe26, Phe75, and Phe78 are well resolved from the rest of the phenylalanine resonances (between 7..2 and 7.4 ppm). The chemical shift dispersion of these resonances is due mainly to ring current shifts as a result of interactions between the six phenylalanine rings, since there are no other aromatic residues in the turkey TR_1C fragment. NOESY cross-peaks are observed between Phe75δ and Phe26δ, and between Phe78δ and Phe75 δ- and ϵ-hydrogens, confirming that these residues are in close proximity, forming an aromatic cluster.

The NOESY cross-peaks observed between various hydrophobic side chains summarized in Table II suggest that helices A, B, and D are in close proximity in metal-free TR_1C; however, no long-range connectivities involving residues in helix C have been observed. The NOESY cross-peaks observed between the Ile37 γ- and δ-CH_3 groups and side chain hydrogens of Phe78, Phe29, Phe26, Val45, and Leu42 suggest that these residues form a hydrophobic core at the interface between helices A, B, and D. Further evidence for formation of a stable "hydrophobic core" between the helices can be observed from the series of 1D spectra shown in Figure 6. The Phe26δ resonance at 6.6 ppm shifts to 6.5 ppm as the temperature is reduced from 30 to 1 °C. The peak broadens to a maximum at 10 °C and then narrows again as the temperature is further reduced. We propose that Phe26 is undergoing ring-flipping in fast exchange on the chemical shift time scale above 30 °C, and moves through intermediate exchange as the temperature is lowered, then into slow exchange below 5 °C. This would be consistent with this

Table II: Long-Range NOE Connectivities Observed between Side Chains of Hydrophobic Residues in the TR_1C Fragment of Turkey Skeletal Muscle TnC in the Absence of Calcium

residues involved		between helices
	From Phe Rings	
Phe22	Leu49	A and B
Phe26	Ile37, Ile73	
	Phe75	A and D
Phe29	Ile37	
	Val45	A and B
Phe75	Phe22, Phe26, Phe78, Leu79	A and D
Phe78	Phe22	A and D
	Leu42, Val45	B and D
	Phe75, Ile37	
	From Upfield-Shifted Methyls	
Ile37	Val45, Leu42, Phe26, Phe29, Phe78	
Val45	Phe29	A and B
	Phe78	B and D

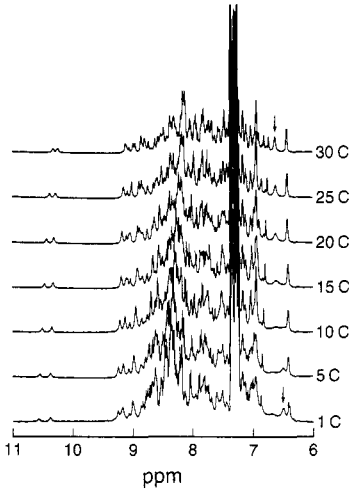

FIGURE 6: Amide and aromatic regions of 1D ^{1}H-NMR spectra of 0.9 mM TR_1C fragment of turkey skeletal TnC in 10 mM KH_2PO_4, 50 mM KCl, and 10% ^2H_2O at pH 6.5 and various temperatures. The position of the Phe26δ resonance is indicated by an arrow on the first and last spectra.

phenylalanine ring being sterically restricted by interactions with other side chains. Broadening of the Phe26ϵ resonance is not observed, implying that its chemical shift is very similar in the two orientations. The Phe26 aromatic hydrogens have NOE cross-peaks with Asp36 and Asp74 CαH resonances as well as with Ile37 δ- and γ-CH_3 groups, which suggests that the Phe26 ring is close to the β-sheet as well as being involved in the hydrophobic core.

The global fold expected for the TR_1C fragment of TnC in solution in the absence of metal ions is shown in Figure 7 which represents a single well-converged structure generated by the program DG-II (Havel, 1991) using the observed NOE connectivities. This structure is consistent with all the NOE connectivities observed, but as mentioned previously, we have observed no long-range connectivities involving residues in helix C, so at the moment its position is constrained only by the short linker from helix B and by formation of the β-sheet between the two calcium binding loops. Even at this level, we can see the packing of helices A, B, and D to form the hydrophobic core mentioned above.

DISCUSSION

Four helical regions are defined for the TR_1C fragment—from Glu16 to Asp27, from Glu41 to Gly50, from Lys55 to Val65, and from Phe75 to Met86—based on the

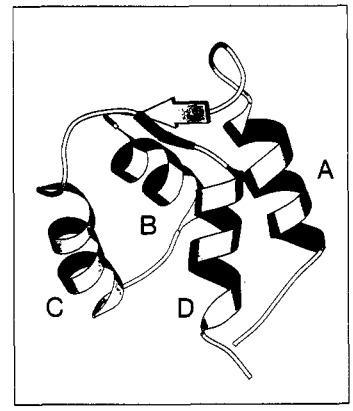

FIGURE 7: Global fold of the TR_1C fragment of turkey skeletal TnC in the absence of calcium. Backbone coordinates of a single well-converged structure generated by the program DG-II (Havel, 1991) using the NOE connectivities reported here are displayed using the program MOLSCRIPT (Kraulis, 1991).

observed CαH–NH(i,i+3) NOE cross-peaks [and some CαH–CβH(i,i+3) ones] and slowly exchanging amide hydrogens. Long-range NOESY cross-peaks are observed consistent with formation of a short antiparallel β-sheet between residues Asp36 to Ser38 in site I and between Thr72 to Asp74 in site II. In the crystal structures of avian TnC (Herzberg & James, 1988), helix A includes residues 16–28, helix B residues 39–48, helix C residues 55–65, and helix D residues 75–86. Hydrogen bonds are found between Gly35 and Phe75, Ile37 and Ile73, and Thr39 and Gly71. There is an additional N-terminal helix from residues 3 to 13, but this is not present in the TR_1C fragment. It thus appears that the secondary structure of the TR_1C fragment in solution in the absence of calcium is very similar to that of the corresponding region in the crystal structure of turkey skeletal TnC, with two helix–loop–helix motifs joined by a short β-sheet between the two calcium binding loops. In the crystal structure of TnC, helix B is kinked, and both Thr39 and Glu41 have distorted ϕ and ψ angles. Strynadka and James (1989) describe a type III β-turn between the carbonyl oxygen of Ser38 and the NH of Glu41, followed by a type I β-turn between the carbonyl oxygen of Thr39 and the NH of Leu42, before the regular α-helix begins at Gly43. They suggest that the bend in helix B allows residues Leu42, Val45, and Met46 to interact with the hydrophobic surfaces of helices A and D. This may also be true in solution since we see NOESY cross-peaks from residues Leu42 and Val45 of helix B to residues in helices A and D. The NMR results also suggest that in solution helix B has two extra residues at the C-terminus which makes the linker between helices B and C two residues shorter than in the crystal structure. This very short linker of only four residues will restrict the relative orientation of the two helix–loop–helix motifs.

The most interesting observation is that the two calcium binding sites are different from each other. Site II has the secondary structure consistent with a classical "EF-hand" calcium-filled site (Strynadka & James, 1989) with helix C ending one residue before the first calcium ligand (Asp66) and helix D starting one residue after the last residue in the short β-strand (Asp74). In contrast, helix A in site I ends three residues before the first calcium ligand (Asp30), and helix B starts three residues after the last residue in the short β-strand (Ser38). It therefore appears that site I has a different preformed secondary structure from site II in the absence of calcium. The increase in helicity of TnC upon binding of calcium to the lower affinity sites (Johnson & Potter, 1978) may reflect the extension of helices A and B toward the calcium loop in the calcium-bound state to form a normal helix–loop–

helix motif. The difference in structure of the two calcium binding sites may also be reflected in a difference in their affinity for calcium.

We observe NOESY cross-peaks between residues in helices A and B, and A and D, suggesting that these helices are in close proximity in metal-free TR_1C. The NOESY cross-peaks observed between the Ile37 γ- and δ-CH_3 groups and side chain hydrogens of Phe78, Phe29, Phe26, Val45, and Leu42 suggest that these residues form a hydrophobic core at the interface between helices A, B, and D and formation of this core is supported by the restricted mobility observed for the Phe26 ring. In the crystal structure of the whole TnC molecule (Herzberg & James, 1988), helices A and B and helices C and D are almost antiparallel to each other. These four helices and the N-terminal helix are loosely packed around a hydrophobic core consisting of Phe26, Phe78, Leu79, Met82, Gln85, Val45, and Met46.

The global fold consistent with the NMR data suggests that helices A, B, and D are loosely packed around a hydrophobic core but exhibit little contact with helix C as reflected by the absence of long-range NOE cross-peaks involving side chains of residues in this helix. Our preliminary NMR structure of the TR_1C fragment is very similar in both secondary structure and global fold to the corresponding region of the crystallographic structure of whole TnC, despite the difference in pH between the two studies, the absence of the N-helix in the TR_1C fragment, and the removal of the whole C-domain. This lack of effect of the C-domain on the structure of the calcium binding sites in the N-domain is also reflected in the similarity of our chemical shift assignments for the TR_1C fragment with several that Tsuda et al. (1990) obtained for the metal-free N-domain in whole TnC.

The preliminary structure of the TR_1C fragment of turkey skeletal TnC presented here appears to be rather loosely packed, and work is presently under way to determine whether this is due to flexibility of this domain in the absence of metal ions or is a consequence of the limited NOE data set available for this molecule. The sequence-specific ^{1}H-NMR assignments reported here will also be used to define at the atomic level changes accompanying calcium binding to the N-terminal domain of skeletal TnC. Determination of the structure of this domain in the calcium-bound form and comparison of the two structures should lead to an understanding of how calcium binding to TnC triggers the events which result in muscle contraction.

ACKNOWLEDGMENT

We thank Linda F. Golden for purifying the turkey skeletal TnC used for making the TR_1C fragment, Gerry McQuaid for upkeep of the spectrometers, and Dr. Frank Sönnichsen for help with using DG-II to determine the global fold. Helpful discussions with Drs. Frank D. Sönnichsen and Gary S. Shaw were also much appreciated.

REFERENCES

Akke, M., Drakenberg, T., & Chazin, W. (1992) *Biochemistry 31*, 1011–1020.

Babu, Y. S., Sack, J. S., Greenhough, T. J., Bugg, C. E., Means, A. R., & Cook, W. J. (1985) *Nature 315*, 37–40.

Barbato, G., Ikura, M., Kay, L. E., Pastor, R. W., & Bax, A. (1992) *Biochemistry 31*, 5269–5278.

Brito, R. M. M., Putkey, J. A., Strynadka, N. C. J., James, M. N. G., & Rosevear, P. R. (1991) *Biochemistry 30*, 10236–10245.

Brown, S. C., Weber, P. L., & Mueller, L. (1988) *J. Magn. Reson. 77*, 166–169.

Chazin, W. J., Kordel, J., Drakenberg, T., Thulin, E., Brodin, P., Grundstrom, T., & Forsén, S. (1989) *Proc. Natl. Acad. Sci. U.S.A. 86*, 2195–2198.

Drabikowski, W., Dalgarno, D. C., Levine, B. C., Gergely, J., Grabarek, Z., & Leavis, P. C. (1985) *Eur. J. Biochem. 151*, 17–28.

Drakenberg, T., Forsén, S., Thulin, E., & Vogel, H. J. (1987) *J. Biol. Chem. 262*, 672–678.

Fujimori, K., Sorsensen, M., Herzberg, O., Moult, J., & Reinach, F. C. (1990) *Nature 345*, 182–184.

Grabarek, Z., Drabikowski, W., Vinkuov, L., & Lu, R. C. (1981) *Biochim. Biophys. Acta 671*, 227–233.

Grabarek, Z., Tan, R.-Y., Wang, J., Tao, T., & Gergely, J. (1990) *Nature 345*, 132–135.

Havel, T. F. (1991) *Prog. Biophys. Mol. Biol. 56*, 43–78.

Heidorn, D. B., & Trewhella, J. (1988) *Biochemistry 27*, 909–915.

Herzberg, O., & James, M. N. G. (1985) *Nature 313*, 653–659.

Herzberg, O., & James, M. N. G. (1988) *J. Mol. Biol. 203*, 761–779.

Herzberg, O., Moult, J., & James, M. N. G. (1986) *J. Biol. Chem. 261*, 2638–2644.

Ikura, M., Kay, L. E., & Bax, A. (1990) *Biochemistry 29*, 4659–4667.

Ikura, M., Kay, L. E., Krinks, M., & Bax, A. (1991a) *Biochemistry 30*, 5498–5504.

Ikura, M., Spera, S., Barbato, G., Kay, L. E., Krinks, M., & Bax, A. (1991b) *Biochemistry 30*, 9216–9228.

Ikura, M., Clore, G. M., Gronenborn, A. M., Zhu, G., Klee, C. B., & Bax, A. (1992) *Science 256*, 632–638.

Johnson, J. D., & Potter, J. D. (1978) *J. Biol. Chem. 253*, 3775–3777.

Kördel, J., Skelton, N. J., Akke, M., Palmer, A. G., III, & Chazin, W. J. (1992) *Biochemistry 31*, 4856–4866.

Kraulis, P. J. (1991) *J. Appl. Crystallogr. 24*, 946–950.

Krudy, G. A., Brito, R. M. M., Putkey, J. A., & Rosevear, P. R. (1992) *Biochemistry 31*, 1595–1602.

Leavis, P. C., Rosenfeld, S. S., Gergely, J., Grabarek, Z., & Drabikowski, W. (1978) *J. Biol. Chem. 253*, 5452–5459.

Linse, S., Teleman, O., & Drakenberg, T. (1990) *Biochemistry 29*, 5925–5934.

McCubbin, W. D., Oikawa, K., Sykes, B. D., & Kay, C. M. (1982) *Biochemistry 21*, 5948–5956.

Pearlstone, J. R., Borgford, T., Chandra, M., Oikawa, K., Kay, C. M., Herzberg, O., Moult, J., Herklotz, A., Reinach, F., & Smillie, L. B. (1992) *Biochemistry 31*, 6545–6553.

Potter, J. D., & Gergely, J. (1975) *J. Biol. Chem. 250*, 4628–4633.

Satyshur, K. A., Rao, S. T., Pyzalska, D., Drendel, W., Greaser, M., & Sundaralingam, M. (1988) *J. Biol. Chem. 263*, 1628–1647.

Sheng, Z., Strauss, W. L., Francois, J.-M., & Potter, J. D. (1990) *J. Biol. Chem. 265*, 21554–21560.

Skelton, N. J., Forsén, S., & Chazin, W. (1990) *Biochemistry 29*, 5752–5761.

Strynadka, N. C. J., & James, M. N. G. (1989) *Annu. Rev. Biochem. 58*, 951–998.

Sundaralingam, M., Bergstrom, R., Strasburg, G., Rao, S. T., Roychowdhury, P., Greaser, M., & Wang, B. C. (1985) *Science 227*, 945–948.

Tsuda, S., Hasegawa, Y., Yoshida, M., Yagi, K., & Hikichi, K. (1988) *Biochemistry 27*, 4120–4126.

Tsuda, S., Ogura, K., Hasegawa, Y., Yagi, K., & Hikichi, K. (1990) *Biochemistry 29*, 4951–4958.

Wagner, G., & Wüthrich, K. (1982) *J. Mol. Biol. 155*, 347–366.

Wishart, D. S., Sykes, B. D., & Richards, F. M. (1991) *FEBS Lett. 293*, 72–80.

Wüthrich, K. (1986) *NMR of Proteins and Nucleic Acids*, Wiley, New York.

Zot, A. S., & Potter, J. D. (1987) *Annu. Rev. Biophys. Biophys. Chem. 16*, 535–539.